IJE TRANSACTIONS C: Aspects Vol. 29, No. 6, (June 2016)

International Journal of Engineering

Journal Homepage: www.ije.ir

Post-critical Behavior of Three-dimensional Composite Beams Near the Autoparametric Resonance under Flapwise Excitation

M. Eftekhari*

Department of Mechanical Engineering, Shahid Bahonar University of Kerman, Kerman, Iran

PAPER INFO

Paper history:
Received 21 December 2015
Received in revised form 09 March 2016
Accepted 02 June 2016

Keywords:
Composite Beam
Flapwise Excitation
Autoparametric Resonance
Periodic Motions

ABSTRACT

The bifurcation analysis of a symmetrically composite beam subjected to harmonic flapwise base excitation is studied when the ratio of flapwise and chordwise internal resonances is 1:2. Results are obtained by the numerical solution of modulation equations. In previous works,the modulation equations did not exihibit any symmetric properties and the modified equations with symmetric properties are studied in this paper. Chracteristics of the response are investigated in terms of time history, phase portraits diagrams and bifurcation diagram of poincare maps. It is observed that periodic and multi-periodic motions, jump and stable motion are appeared near the internal and external tunnig frequency parameters.

***doi**: 10.5829/idosi.ije.2016.29.06c.00*

NOMENCLATURE

		$u(s,t), v(s,t), w(s,t)$	Beam neutral axis deflection along *x*,*y* and *z* axes
xyz	Inertial coordinate system	$c_i (i = u, v, w, \phi)$	Damping coefficients
$\xi\eta\zeta$	Principle axes coordinate system of beam cross-section at position *s*	$D_{11}, D_{22}, D_{33}, D_{13}$	Bending and stiffness rigidities
m	Mass of the beam per unit length *l*	$Q_i (i = u, v, w, \phi)$	External forces
J_ξ, J_η, J_ζ	Nondimensional mass moments mass moments of inertia	$e, \varepsilon_{\xi\eta}, \varepsilon_{\xi\zeta}$	Axial and shear strains at the point $(\xi,0,0)$ along the elastic axis
$E_i (i = 1,2,3)$, G_{12}, G_{13}, G_{23}	Elastic and shear modulus	ρ_0	Density (lbm/ft^3)
$\ell(s,t)$	Lagrangian density	$\phi(s,t)$	Beam neutral axis rotation angle about ξ axis
$\rho_\xi, \rho_\eta, \rho_\zeta$	Curvatures	l	Length of beam (ft)
$\upsilon_{12}, \upsilon_{13}, \upsilon_{23}$	Poisson's ratios	b	Width of cross section of beam (in)
h_k	Lamina thickness (in)	h	Thickness of cross section of beam (in)

1. INTRODUCTION

The motivation of the present paper arises from the need for further understanding the dynamic behavior of a composite beam. Laminated beams find applications in a variety of structural components such as helicopter rotor blades, mast antennas, flexible satellites, robot arms, towers, long-span bridges, etc. In nonlinear systems, when the system parameters are changed, the dynamic behavior is varied from equilibrium to limit cycle as a regular attractor. In certain regions of the parameter space, the regular attractors change to strange attractors. In these regions, chaotic motions occure. For

*Corresponding Author's Email: *mojtaba.eftekhari59@gmail.com* (M. Eftekhari)

Please cite this article as: M. Eftekhari, Post-critical Behavior of Three-dimensional Composite Beams Near the Autoparametric Resonance under Flapwise Excitation, International Journal of Engineering (IJE), TRANSACTIONS C: Aspects Vol. 29, No. 6, (June 2016)

chaos detection, quality tools such as time history plots, phase-plane projections, frequency spectral, and bifurcation diagrams of Poincaré maps are used [1-3]. For the quantification of chaos, some tools such as Lyapunov exponents and fractal dimension (Lyapunov dimension) are widely used.

Many researchers have investigated the linear and nonlinear vibration of beams [4-8]. Cao and Zhang studied the chaotic behavior and bifurcation of a string-beam system [9]. The divergence and flutter of laminated composite beam which is subjected to a combination of conservative and non-conservative follower loads have been performed by Goyal and Kapania [10]. Egidio has utilized the multiple scale method to investigate the post-critical behavior of a planar beam equipped with a lumped visco-elastic device [11]. In that study, stability of fixed points, Hopf bifurcation, duoble zero and divergence-Hopf bifurcation have been presented. Kim has applied the finite element method to study the dynamic response of damped laminated beam [12]. Results indicated that the variation of fiber orientation, different boundary conditions and damping can influence on the instability region of divergence-flutter system. Bifurcation analysis of a visco-elastic beam has been performed by Luongo and Dannibale [13]. The analysis contains the codimension-1 and codimension-2 bifurcation and post-critical behavior near the Hopf bifurcation. Daqaq have studied the dynamic response of a piezoelectrically actuated cantilever beam which has been subjected to delayed feedback [14]. The gain of feedback delay, the external excitation amplitude and excitation frequency can be effect on the periodic, quasi-periodic and chaotic motion of beam. Lacarbonara et.al have investigated the nonlinear response of an imperfect beam under base acceleration excitation [15]. Frequency and forced responses, Hopf and homoclinic bifurcations have presented by taking in to account internal and external resonances. In recent years, stability and dynamic behavior of micro-beams are investigated [16, 17].

Pai and Nayfeh have been derived the nonlinear equations of symmetrically composite beam [18]. However , as mentioned in the thesis of Arafat [19], their modulation equations did not exhibit any symmetric properties and did not reflect the conservative nature of composite beam in the absence of damping. Therefore, the results were incorrect. The equations have been derived by Arafat [19] using the variational approach. Arafat applied directly the method of multiple scales on equations to obtain the modulation equations and did not perform further analysis.

The stability of fixed points of modulation equations are investigated by Eftekhari et.al. [20]. Physically, a fixed point corresponds to an equilibrium position of a system. The stability of a fixed point is determined by investigating the eigenvalues of the Jacobian matrix of the right-hand sides of modulation equations. When all of the eigenvalues have nonzero real parts, the corresponding fixed point is called as hyperbolic fixed point, irrespective of the values of the imaginary parts; otherwise, it is called non-hyperbolic fixed point. There are three types of hyperbolic fixed points: sinks, sources and saddle points. A pseudo arclength scheme is used to find the branches of equilibrium solutions. The fixed points of a system can lose stability due to saddle-point bifurcations or Hopf bifurcations.

In this paper, the modified modulation equations are solved by Runge-Kutta method. Dynamic behavior of composite beam in the present of 2-1 internal resonance is studied. Bifurcation diagrams of Poincare maps of deflection beam are presented versus the internal and external dettuning parameters.

The rest of this paper is organized as follows. In section 2, the non-dimensional equations of cantilever beam subjected to the harmonic base excitation is rewritten. In section 3, bifurcation diagrams of Poincare maps for the steady-state deflection amplitudes of beam are analyzed as well as time history, phase portraits diagrams. Results contain stable, periodic and multi-periodic motions.

2. NONDIMENSIONAL GOVERNING EQUATIONS

The nonlinear equations of motion for the composite beam as shown in Figure 1 are derived using the extended Hamilton's principle as [19]:

$$\int_{t1}^{t2}(\delta L+\delta w_e)dt=0, \tag{1}$$

where δL and δw_e are the variation of the Lagrangian and virtual work of non-conservative force, respectively. Following Arafat [19], by introducing the Lagrangian density $\ell(s,t)$ and Lagrange multiplier $\lambda(s,t)$ to enforce inextensionality conditions, the virtual work of non-conservative force and the Lagrangian of the beam can be obtained as:

$$\delta w_e=\int_0^l\{(Q_u-c_u\dot{u})\delta u+(Q_v-c_v\dot{v})\delta v+(Q_w-c_w\dot{w})\delta w+(Q_\phi-c_\phi\dot{\phi})\delta\phi\}ds, \tag{2}$$

$$\delta L=\int_0^l\delta\ell(s,t)ds, \tag{3}$$

$$\ell(s,t)=(1/2)\{m(\dot{u}^2+\dot{v}^2+\dot{w}^2)+(J_\xi\omega_\xi^2+J_\eta\omega_\eta^2+J_\zeta\omega_\zeta^2)-\mathrm{E}^T[k]\mathrm{E}+\lambda(1-(1+u')^2-v'^2-w'^2)\}, \tag{4}$$

where, $\mathrm{E},[k]$ are defined as [19]:

$$\mathrm{E}=\{e\quad \varepsilon_{\xi\eta}\quad \varepsilon_{\zeta\xi}\quad \rho_\xi\quad \rho_\eta\quad \rho_\zeta\}^T,$$
$$[k]=\begin{bmatrix}A & B\\ B^T & D\end{bmatrix} \tag{5}$$

The matix $[k]$ is computed for the composite beam [19].

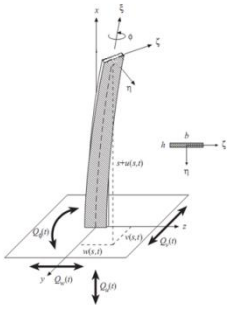

Figure. 1. A schematic of cantilever beam [19].

Substituting Equations (2-3) in Equation (1), and noting the fact that $\delta u(s,t), \delta v(s,t), \delta w(s,t), \delta\phi(s,t)$ and $\delta u(l,t), \delta v(l,t), \delta w(l,t), \delta\phi(l,t)$ are arbitrary, the governing equations and boundary conditions are obtained. Dimensionless equations are derived in terms of the following parameters [19]:

$$v^* = \frac{v}{l}, w^* = \frac{w}{l}, s^* = \frac{s}{l}, c_v^* = \frac{c_v l^2}{\sqrt{mD_{33}}}, \beta_{33} = 1,$$
$$c_\phi^* = \frac{c_\phi l^2}{\sqrt{mD_{33}}}, \beta_{11} = \frac{D_{11}}{D_{33}}, J_\zeta^* = \frac{J_\zeta}{mL^2}\beta_{22} = \frac{D_{22}}{D_{33}}, \beta_{13} = \frac{D_{13}}{D_{33}},$$
$$J_\eta^* = \frac{J_\eta}{mL^2}, J_\xi^* = \frac{J_\xi}{mL^2}, Q_w^* = \frac{l^3}{D_{33}}Q_w, Q_v^* = \frac{l^3}{D_{33}}Q_v, \quad (6)$$
$$Q_\phi^* = \frac{l^3}{D_{33}}Q_\phi, Q_u^* = \frac{l^3}{D_{33}}Q_u, t^* = \sqrt{\frac{D_{33}}{ml^4}}\,t, c_w^* = \frac{c_w l^2}{\sqrt{mD_{33}}},$$

The forcing terms, damping terms, and both quadratic and cubic nonlinear terms are assumed to be of order ε. By dropping the asterisks for convenience, the nondimensional equations and associated boundary conditions are rewritten as follows [19]:

$$\ddot{v} + \varepsilon c_v\dot{v} + \beta_{33}v^{iv} + \beta_{13}\phi''' - J_\zeta\ddot{v}'' = \varepsilon\{Q_v(t) - [v'(s-1)]'Q_u(t) + H_v(s,t)\}, \quad (7)$$

$$\ddot{w} + \varepsilon c_w\dot{w} + \beta_{22}w^{iv} - J_\eta\ddot{w}'' = \varepsilon\{Q_w(t) - [w'(s-1)]'Q_u(t) + H_w(s,t)\}, \quad (8)$$

$$J_\xi\ddot{\phi} + \varepsilon c_\phi\dot{\phi} - \beta_{11}\phi'' - \beta_{13}v''' = \varepsilon\{Q_\phi(t) + H_\phi(s,t)\}, \quad (9)$$

The corresponding boundary conditions are:

$$v = 0, v' = 0, w = 0, w' = 0, \phi = 0, \ at\ s = 0, \quad (10)$$

$$\beta_{33}v'' + \beta_{13}\phi' = \varepsilon(B_{v1}(t)), \ at\ s = 1, \quad (11)$$

$$\beta_{33}v''' + \beta_{13}\phi'' - J_\zeta\ddot{v}' = \varepsilon(B_{v2}(t)), \ at\ s = 1, \quad (12)$$

$$\beta_{22}w'' = \varepsilon(B_{w1}(t)), \ at\ s = 1, \quad (13)$$

$$\beta_{22}w''' - J_\eta\ddot{w}' = \varepsilon(B_{w2}(t)), \ at\ s = 1, \quad (14)$$

where, the functions $H_v(s,t), H_w(s,t), H_\phi(s,t)$ and $B_{v1}(t), B_{v2}(t), B_{w1}(t), B_{w2}(t), B_{\phi1}(t)$ are defined in Equations (15-22) [19].

$$H_v(s,t) = -\beta_{11}(\phi'w' + v''w'^2)'' - (\beta_{22} - \beta_{33})(\phi^2v'' - \phi w'')'' - \beta_{33}[v'(v'v'')' + v'(w'w'')']' + \beta_{13}[(1/2)(\phi'\phi^2)' - (w'w'')'\phi - (2v''w')' - (1/2)v'^2\phi'']' + J_\xi\frac{\partial}{\partial t}(\dot{\phi}w' + \dot{v}'w'^2)' - (1/2)\{v'\int_1^s[\frac{\partial^2}{\partial t^2}\int_0^s(v'^2 + w'^2)]ds\}', \quad (15)$$

$$H_w(s,t) = \beta_{11}(\phi'v'' + v''^2w')'' + (\beta_{22} - \beta_{33})(\phi^2w'' + \phi v'')'' - \beta_{22}[w'(w'w'')'] - \beta_{33}[w'(v'v'')']' + \beta_{13}[v''^2 - (\phi\phi')' - w'(\phi v')'']' - J_\xi(\dot{\phi}\dot{v}' + \dot{v}'^2w')' - (1/2)\{w'\int_1^s[\frac{\partial^2}{\partial t^2}\int_0^s(v'^2 + w'^2)]ds\}', \quad (16)$$

$$H_\phi(s,t) = \beta_{11}(v''w')' + (\beta_{22} - \beta_{33})(w''v'' - \phi v''^2 + \phi w''^2) + \beta_{13}[(1/2)(v'^2v'')' - (1/2)(\phi^2v''') + v'(w'w'')' + \phi w'''] - J_\xi\frac{\partial}{\partial t}(\dot{v}'w'), \quad (17)$$

$$B_{v1}(t) = -\beta_{11}(v''w'^2 + \phi'w') - (\beta_{22} - \beta_{33})(\phi^2v'' - \phi w'' - v'w'w'') + \beta_{13}((1/2)\phi^2\phi' - (1/2)v'^2\phi' - \phi w'w'' - 2v''w'), \quad (18)$$

$$B_{v2}(t) = -\beta_{11}(v''w'^2 + \phi'w') - (\beta_{22} - \beta_{33})(\phi^2v'' - \phi w'')' - \beta_{33}[v'(v'v'')' + v'(w'w'')'] + \beta_{13}((1/2)(\phi^2\phi')' - (1/2)v'^2\phi'' - \phi(w'w'')' - 2(v''w')') + J_\xi\frac{\partial}{\partial t}(\dot{\phi}w' + \dot{v}'w'^2), \quad (19)$$

$$B_{w1}(t) = (\beta_{22} - \beta_{33})(\phi^2w'' + \phi v'') - \beta_{13}(\phi\phi' + (\phi v')'w'), \quad (20)$$

$$B_{w2}(t) = \beta_{11}(w'v''^2 + v''\phi') - (\beta_{22})[w'(w'w'')'] - (\beta_{33})[w'(v'v'')'] - J_\xi(w'\dot{v}'^2 + \dot{\phi}\dot{v}') + (\beta_{22} - \beta_{33})(\phi^2w'' + \phi v'')' - \beta_{13}[w'(\phi v')'' + (\phi\phi')' - v''^2], \quad (21)$$

$$B_{\phi1}(t) = -\beta_{11}(v''w') + \beta_{13}((1/2)\phi^2v'' - (1/2)v'^2v'' - \phi w'' - v'w'w''), \quad (22)$$

By applying the method of multiple scales to Equations (7-14), the displacments v, w, ϕ can be express in terms of different time scales (T_0, T_1) as:

$$v(s,t) = v_0(s,T_0,T_1) + \varepsilon v_1(s,T_0,T_1) + \ldots \quad (23)$$

$$w(s,t) = w_0(s,T_0,T_1) + \varepsilon w_1(s,T_0,T_1) + \ldots \quad (24)$$

$$\phi(s,t) = \phi_0(s,T_0,T_1) + \varepsilon\phi_1(s,T_0,T_1) + \ldots \quad (25)$$

where ε is a book keeping parameter that will be set to unity at the end of the analysis. By substituting Equations (23-25) in to Equations (7-14) and eliminating all secular terms, the modulation equations are obtained as follows [19]:

$$2i\omega\Gamma_1 A' = (2i\omega\Gamma_2)A - \Gamma_3\overline{A}Be^{2i\omega\delta T_1} - 2\Gamma_4 AB\overline{B} - 3\Gamma_5 A^2\overline{A} - \Gamma_6 e^{i\omega\sigma T_1}, \quad (26)$$

$$2i\rho\Lambda_1 B' = (2i\rho\Lambda_2)B - \Lambda_3 A^2 e^{-2i\omega\delta T_1} - 2\Lambda_4 A\overline{A}B - 3\Lambda_5 B^2\overline{B}, \quad (27)$$

In Equations (26) and (27), the parameters $\Gamma_i (i=1..6), \Lambda_i (i=1..5)$ are evaluted for the composite beam as [19]:

$$\Gamma_1 = -1.00005, \Gamma_2 = 0.035232, \Gamma_3 = -41.37849, \Gamma_4 = -20.78901, \Gamma_5 = -39.00110, \Gamma_6 = -0.39149 f_v\Omega^2 \quad (28)$$

$$\Lambda_1 = -1.00008, \Lambda_2 = 0.064994, \Lambda_3 = -20.68924, \Lambda_4 = -20.78901, \Lambda_5 = -9.28130, \quad (29)$$

In Equation (28), $f_v = (1/2)\int_0^1 f\phi_v(s)ds,$. $f, \phi_v(s)$ are the force ampitude of excitation in y direction ($Q_v(t)$) and mode shape of the composite beam in y direction respectively.

The modulation equations are obtained in polar and cartesian forms by the following transformations

$$A = \frac{1}{2}a_1(T_1)e^{i\theta_1(T_1)}, B = \frac{1}{2}a_2(T_1)e^{i\theta_2(T_1)}, \quad \textit{for polar form} \quad (30)$$

$$A = \frac{1}{2}(p_1 - iq_1)e^{i\omega\sigma(T_1)}, B = \frac{1}{2}(p_2 - iq_2)e^{2i\omega(\sigma-\delta)T_1}, \quad \textit{for cartesian form} \quad (31)$$

In polar form

$$a_1' + \hat{\mu}_1 a_1 + S_{13}a_1a_2\sin(\upsilon_1) + \hat{R}_v\sin(\upsilon_2) = 0, \quad (32)$$

$$a_1\upsilon_2' - a_1\omega\sigma + S_{13}a_1a_2\cos(\upsilon_1) + S_{12}a_1a_2^2 + S_{11}a_1^3 + \hat{R}_v\cos(\upsilon_2) = 0, \quad (33)$$

$$a_2' + \hat{\mu}_2 a_2 - S_{23}a_1^2\sin(\upsilon_1) = 0, \quad (34)$$

$$a_2(\upsilon_1' - 2\upsilon_2') + 2a_2\omega(\sigma-\delta) - S_{23}a_1^2\cos(\upsilon_1) + S_{21}a_2a_1^2 + S_{22}a_2^3 = 0, \quad (35)$$

And in cartesian form

$$p_1' = -\omega\sigma q_1 - \hat{\mu}_1 p_1 + S_{13}(p_1q_2 - p_2q_1) + S_{12}(p_2^2 + q_2^2)q_1 + S_{11}(p_1^2 + q_1^2)q_1, \quad (36)$$

$$q_1' = \omega\sigma p_1 - \hat{\mu}_1 q_1 - S_{13}(p_1p_2 + q_1q_2) - S_{12}(p_2^2 + q_2^2)p_1 - S_{11}(p_1^2 + q_1^2)p_1 - \hat{R}_v, \quad (37)$$

$$p_2' = -2\omega(\sigma-\delta)q_2 - \hat{\mu}_2 p_2 + 2S_{23}(p_1q_2) + S_{21}(p_1^2 + q_1^2)q_2 + S_{22}(p_2^2 + q_2^2)q_2, \quad (38)$$

$$q_2' = 2\omega(\sigma-\delta)p_2 - \hat{\mu}_2 q_2 + S_{23}(q_1^2 - p_1^2) - S_{21}(p_1^2 + q_1^2)p_2 - S_{22}(p_2^2 + q_2^2)p_2, \quad (39)$$

where,

$$S_{11} = \frac{-3\Gamma_5}{8\omega\Gamma_1}, S_{12} = \frac{-\Gamma_4}{4\omega\Gamma_1}, S_{13} = \frac{-\Gamma_3}{4\omega\Gamma_1}, S_{21} = \frac{-\Lambda_4}{4\rho\Lambda_1},$$
$$S_{22} = \frac{-3\Lambda_5}{8\rho\Lambda_1}, S_{23} = \frac{-\Lambda_3}{4\rho\Lambda_1}, \hat{\mu}_1 = -\frac{\Gamma_2}{\Gamma_1}, \hat{R}_v = \frac{\Gamma_6}{\omega\Gamma_1}, \quad (40)$$
$$\upsilon_1 = \theta_2 - 2\theta_1 + 2\omega\delta T_1,\ \upsilon_2 = \omega\sigma T_1 - \theta_1, \hat{\mu}_2 = -\frac{\Lambda_2}{\Lambda_1},$$

The detuning parameters σ, δ are defined to express the nearness of the primary and the two-to-one internal resonances as follows:

$$\Omega = \omega(1 + \varepsilon\sigma), \rho = 2\omega(1 + \varepsilon\delta), \quad (41)$$

In Equation (41), Ω is the excitation frequency of $Q_v(t)$, ω is the natural frequency of the composite beam in y direction and torsional motions and ρ is the natural frequency of the composite beam in z direction.

The fixed ponits of Equations (32-35) and (36-39) have been investigated by Eftekhari et al. [20]. Eftekhari et.al have used a pseudo arclength scheme to find the branches of equilibrium solutions [20].

3. RESULTS AND DISCUSSIONS

For numerical simulation, a graphite epoxy composite beam with layup $[10_6^0/45_4^0/90_5^0]_s$ is considered. The geometry and material properties are tabulated in Table 1, which are based on those in [19]. The ecxitation terms in Equations (7-9) are $Q_v = \hat{f}_v\Omega^2\cos(\Omega t), Q_u = Q_\phi = Q_w = 0, \Omega = \omega(1+\varepsilon\sigma)$, $\rho = 2\omega(1+\varepsilon\delta)$). The nondimensional natural frequencies of the first bending and torsional modes of the composite beam are $\omega = 3.34465987, \rho = 6.68906$ Moreover, the Equations (32-35) are solved by Runge-Kutta method and dynamic behavior is investigated in Figures (2-9). The ampitudes are defined as $a_i(i=1,2) = \sqrt{p_i^2 + q_i^2}$ in the following figures.

TABLE 1. Beam properties

$D_{11}=436.23 lb.in^2$ $D_{22}=5547.2 lb.in^2$ $D_{33}=1532.4 lb.in^2$ $D_{13}=252.02 lb.in^2$	$E_1=1.92\times10^7\ psi$ $E_2=E_3=1.56\times10^6\ psi$ $G_{23}=5.23\times10^5\ psi$ $G_{12}=G_{13}=8.20\times10^5\ psi$	$J_\varsigma=5.78704\times10^{-6}$ $J_\eta=3.62192\times10^{-5}$ $J_\zeta=4.20062\times10^{-5}$ $\rho_0=96.1 lbm/\ ft^3$	$\upsilon_{12}=0.24$ $\upsilon_{13}=0.24$ $\upsilon_{23}=0.49$
l =1.5 *ft*	b=0.37526 *in*	$h_k=0.005 in$	$h=0.15 in$

In this study, the dynamic behavior of beam is investigated when the external and internal detuning parameters of ecxitation (σ,δ) are varied. Bifurcation diagrams of poincare maps are studied for the steady-state deflection amplitudes of the beam. Periodic, quasi-periodic, jump and stable motions are investigated in diagrams. As the first step, the accuracy of the numerical results are verified against those reported in [20] and good agreement is obtained as shown in Figure 2. Figures 2(b) and 2(d) are plotted from [16] and are compared with Figures 2(a) and 2(c) which are obtained in this paper. Figure 2(a) shows the bifurcation diagram of poincare maps of beam deflection for $\delta=-0.01$. periodic motions of a_1,a_2 amplitudes are observed in interval $-0.0150\le\sigma\le0.0140$ and jump occurs at $\sigma=0.0800$ for a_1,a_2. Figure 2(b) represents the frequency response of a_1,a_2 amplitudes for $\delta=-0.01$ from [20]. As shown in case (b), Fixed points lose stability through a Hopf bifurcation at $\sigma=\sigma_1=-0.0151,\sigma=\sigma_2=0.0131$. Moreover, by decreasing σ from 0.2 to 0, jump occurs at $\sigma=0.081$ for a_1,a_2. Amplitude values of stable fixed points of a_1,a_2 in case (b), are in good agreement with stable points in case (a). Figures 2(c) and 2(d) show the amplitudes for $\delta=0.1$. Figure 2(d) is represented from [20] and the stable amplitudes of a_1,a_2 are in good agreement with those in Figure 2(c).

Figure 3 shows the bifurcation diagram of poincare maps of beam deflection under increasing σ,δ for $f_v=0.01$. Figure 3(a) presents a_1,a_2 amplitudes for $\delta=-0.1$ and the solution contain a steady state behavior among $-0.2\le\sigma\le0.0750$ and $0.0750\le\sigma\le0.2$. Jump occurs at $\sigma=0.0750$ for a_1,a_2. By changing the δ from -0.1 to -0.01 in Figure 3(b), periodic motions of a_1,a_2 amplitudes are appeared respectively in intervals $-0.0150\le\sigma\le0.0140$ and $-0.0170\le\sigma\le0.0150$. jump occurs at larger value of $\sigma=0.0800$ in comparison to Figure 3(a). stable region is observed in intervals $-0.2\le\sigma\le-0.015,\ 0.0140\le\sigma\le0.0800,0.0800\le\sigma\le0.2$ for a_1 and in intervals $-0.2\le\sigma\le-0.017,\ 0.0150\le\sigma\le0.0800,0.0800\le\sigma\le0.2$ for a_2.

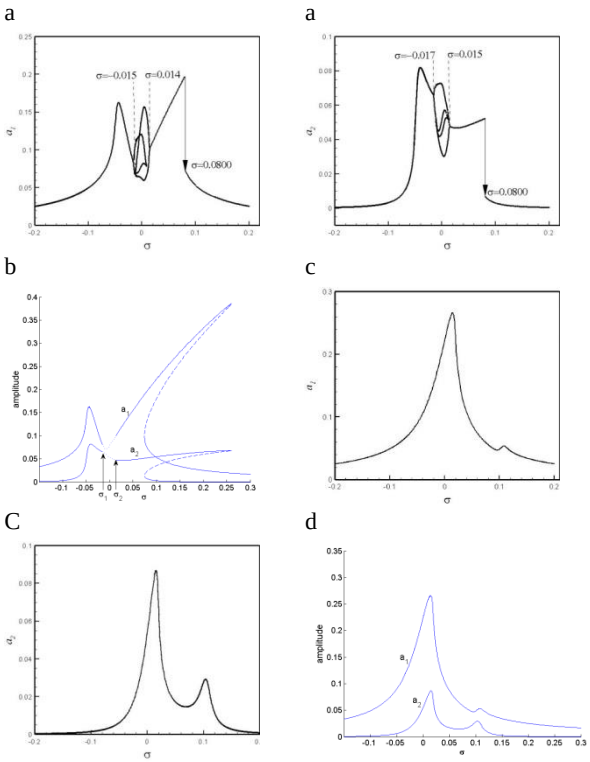

Figure 2. Bifurcation diagram of deflection beam under increasing σ for $f_v=0.01$:(a) numerical results for $\delta=-0.01$ (b) Frequency response for $\delta=-0.01$ [20] , (c) numerical results for $\delta=0.1$, (d) Frequency response for $\delta=0.1$ [20].

As shown in Figure 3(c), increase of the internal resonance detuning parameter to $\delta=0$ changes the periodic motion regions of a_1,a_2 to $-0.0351\le\sigma\le0.0130$ and $-0.0080\le\sigma\le0.0260$ respectively. jump is observed at $\sigma=0.0800$. Figure 3(d) shows the amplitudes for $\delta=0.01$. jump is observed in $\sigma=0.0820$ and periodic motions of a_1,a_2 are shifted to positive values of σ in intervals $0.0050\le\sigma\le0.0350$ and $0.0010\le\sigma\le0.0350$ respectively. Figure 3(e) shows the amplitudes are stable in whole region, when the value of δ is increased to 0.1. maximum value of a_1 amplitude is seen in Figure 3(e) for $\delta=0.1$.

Figure 4(a)-(e) shows the bifurcation diagram of poincare maps of beam deflection for $f_v=0.02$ and different values of δ. Figure 4(a) is plotted for $\delta=-0.1$ and jump occurs in amplitudes at $\sigma=0.1225$. The solution contains the steady state points and jump phenomenon. Figure 4(b) , shows two different regimes of oscilations, explicitly the stable regime, the periodic motions, over the $-0.2\le\sigma\le0.2$ for $\delta=-0.01$. Transition from a stable zone to a periodic bifurcation occurs at $\sigma=-0.0195,0.0490$.

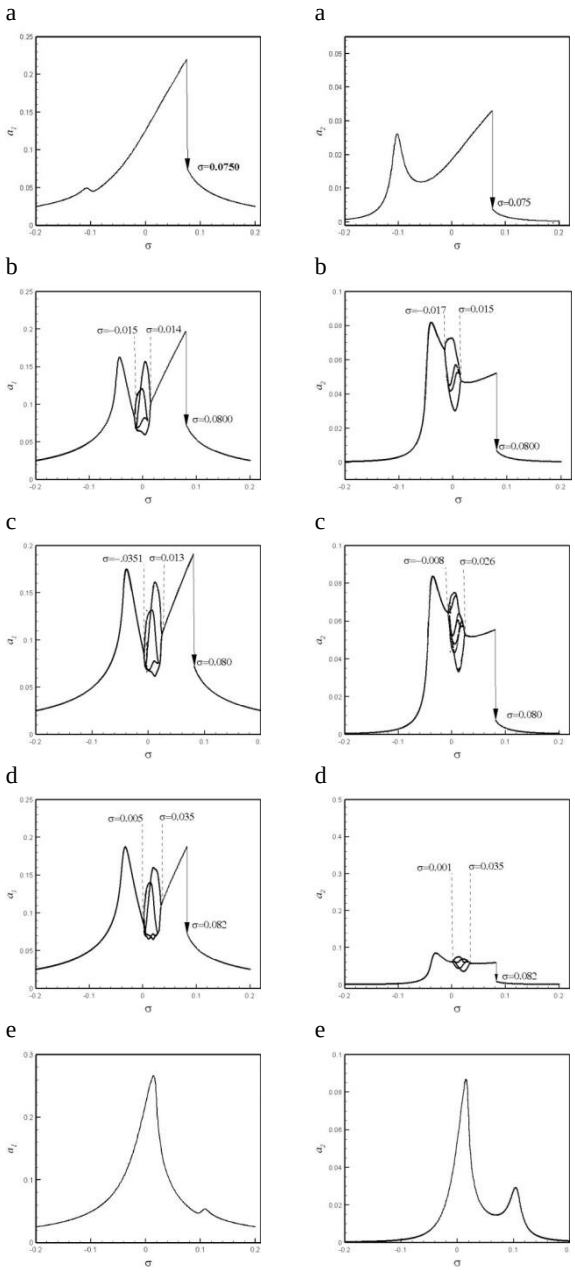

Figure 3. Bifurcation diagram of poincare maps of deflection beam under increasing σ for $f_v = 0.01$: (a) $\delta = -0.1$ (b) $\delta = -0.01$, (c) $\delta = 0$, (d) $\delta = 0.01$, (e) $\delta = 0.1$.

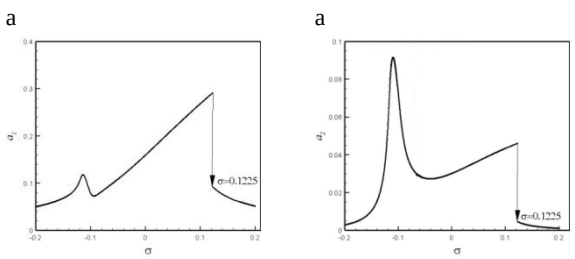

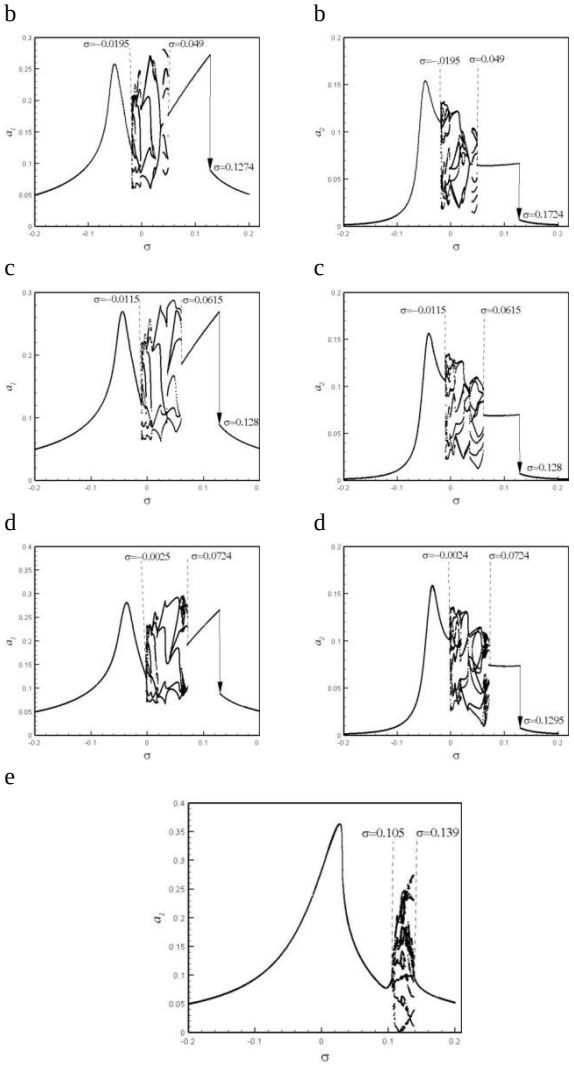

Figure 4. Bifurcation diagram of poincare maps of deflection beam under increasing σ for $f_v = 0.02$: (a) $\delta = -0.1$ (b) $\delta = -0.01$, (c) $\delta = 0$, (d) $\delta = 0.01$, (e) $\delta = 0.1$.

For $\sigma = 0.1274$, jump is illustrated in Figure 4(b). Asymmetric seies of n-period bifurcations is detected at $\sigma = -0.0115, 0.0615$ for perfectly internal resonance detuning parameter $\delta = 0$ in Figure 4(c). jump is shifted to $\sigma = 0.128$ in this figure. For $\delta = 0.01$, as shown in Figure 4(d), Asymmetric seies of n-period bifurcations ocurrs at $\sigma = -0.0025, 0.0724$ for a_1 and $\sigma = -0.0024, 0.0724$ for a_2. jump ocuurs at larger value $\sigma = 0.1295$. The bifurcation diagram is presented for $\delta = 0.1$ in Figure 4(e). As shown in this figure, the beam undergoes stbale motion in the interval $-0.2 \le \sigma \le 0.105$, then it results in a transition to periodic or quasi-periodic motion in interval $0.105 \le \sigma \le 0.139$. Figures (5) and (6) show the time history and phase portraits diagrams for some values of $-0.0025 \le \sigma \le 0.0724$ and

$0.105 \le \sigma \le 0.139$in Figures 4(d) and 4(e) respectively.

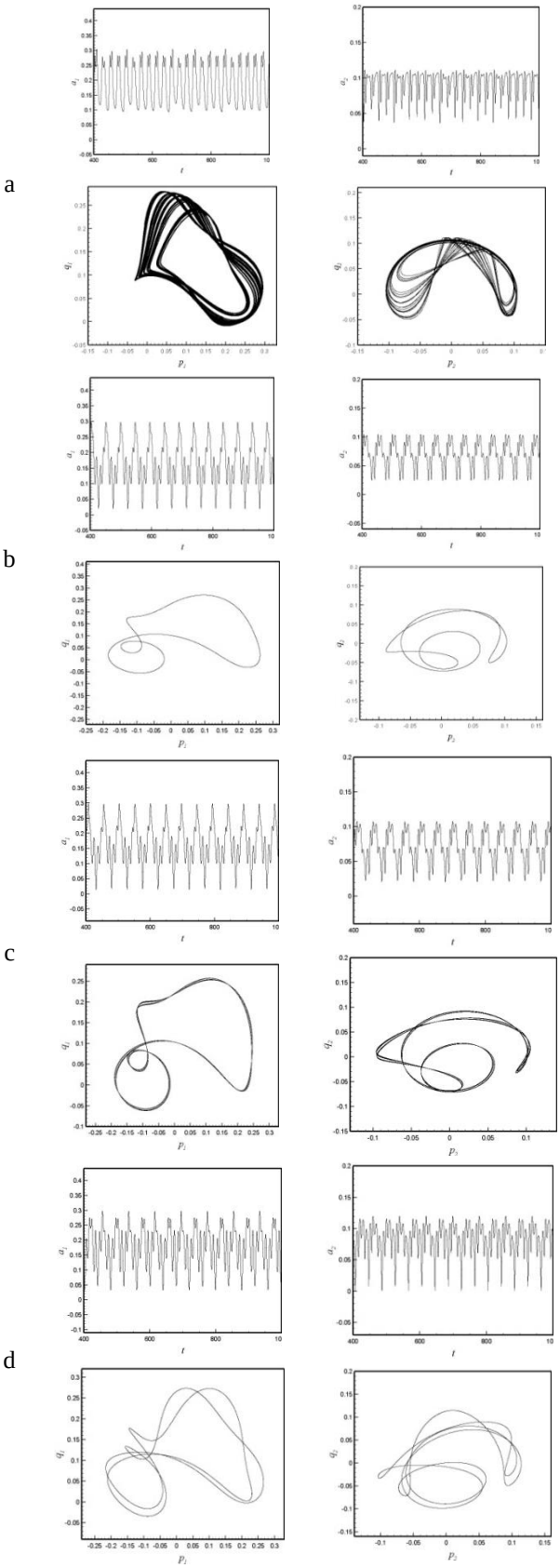

Figure 5. Dynamic responses of beam motion with respect to $f_v = 0.02, \delta = 0.01$ a) $\sigma = -0.002$ b) $\sigma = 0.010$ c) $\sigma = 0.030$ d) $\sigma = 0.040$ e) $\sigma = 0.050$ f) $\sigma = 0.052$ g) $\sigma = 0.064$ h) $\sigma = 0.072$.

As shown in Figures (5) and (6), periodic, quasi-periodic or stable motion may be appeared for different values of $-0.0025 \le \sigma \le 0.0724$ and $0.105 \le \sigma \le 0.139$.

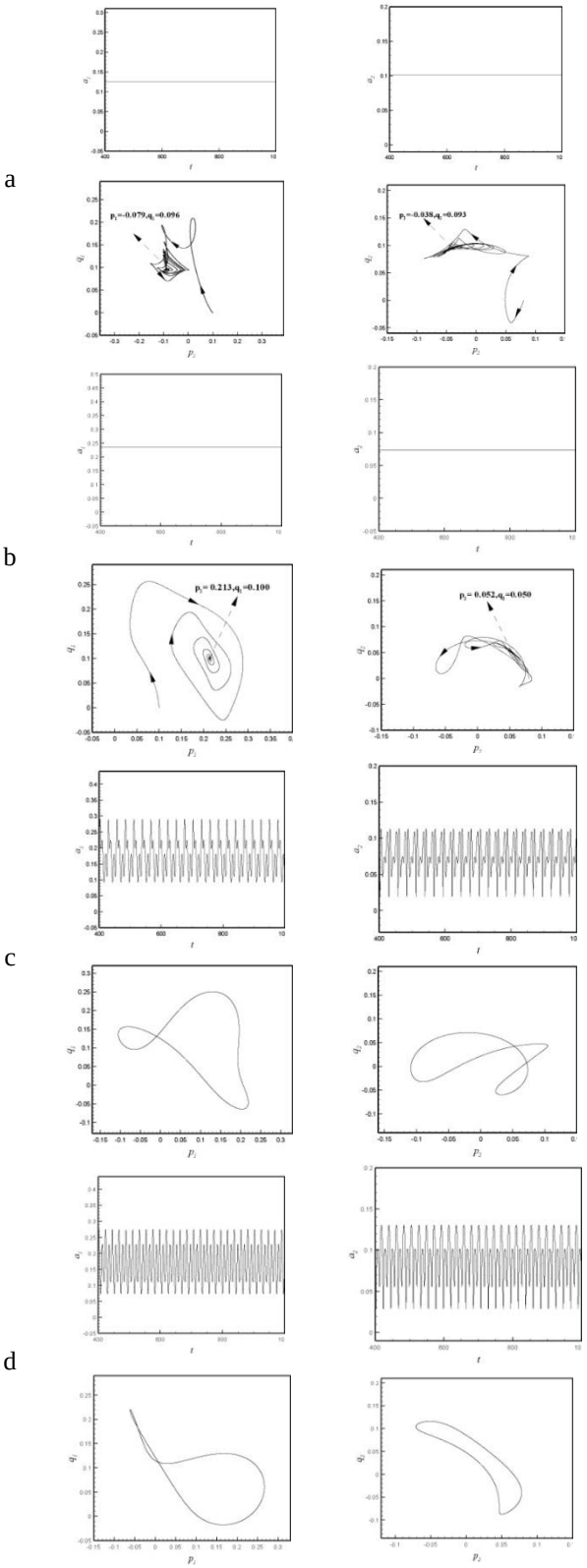

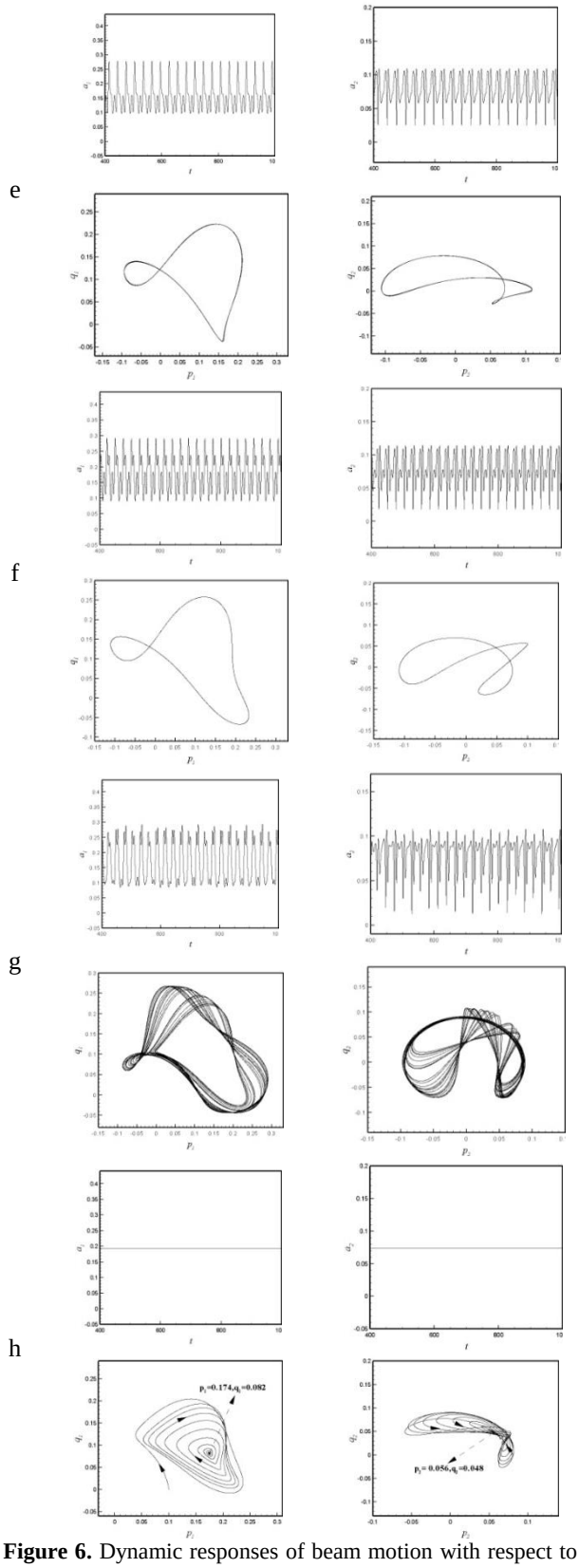

Figure 6. Dynamic responses of beam motion with respect to $f_v = 0.02, \delta = 0.1$ a) $\sigma = 0.015$:,(b) $\sigma = 0.110$ (c) $\sigma = 0.118$, (d) $\sigma = 0.123$, (e) $\sigma = 0.130$, (f) $\sigma = 0.135$ (g) $\sigma = 0.137$ (h) $\sigma = 0.141$.

Figure 5 presents some results in the form of time history, phase portraits diagrams. Figures 5(a)-5(f) show that the responses are periodic for $f_v = 0.02, \delta = 0.01$ and for values of σ which is written in parts a)-f). Figures 5(g) and 5(h) show that the responses are stable for $f_v = 0.02, \delta = 0.01$ and $\sigma = 0.064, 0.072$ respectively. Equiblirium points for a_1, a_2 and $\sigma = 0.064, 0.072$ are respectively $p_1 = -0.054, q_1 = 0.066, p_2 = -0.086, q_2 = 0.002$ and $p_1 = -0.061, q_1 = 0.050, p_2 = -0.074, q_2 = -0.006$.

Figure 6 presents for $f_v = 0.02, \delta = 0.1$. Figure 6(a,b,h) show that the beam motion is stable in whole time domain and equiblirium points are shown in cases (a,b,h) for $\sigma = 0.015, 0.110, 0.141$. Figure 6(c,d,e,f) show that the motion is periodic with one period for $\sigma = 0.118, 0.123, 0.130, 0.135$. Multi-periodic motion is illustrated in Figure 6(g) for $\sigma = 0.137$.

4. CONCLUDING REMARKS

In this paper, the bifurcation diagrams of poincare maps of beam deflection are investigated numerically. Using long-time integration, a bifurcation map of beam response is generated and is presented that for specific values of σ, δ and f_v, the beam response may follow sable, periodic or quasiperiodic motions. The following coclusions are drawn from the numerical results

1)for an arbitrary value of f_v, when the internal resonance detuning parameter (δ) is increased, jump is shifted at higher values of σ and periodic motion is appeared in amplitudes.

2)saturation is appeared in amplitude versus δ digrams for negetive value of σ.

3)when the forcing amplitude is increased, the periodic and multi-periodic motions are releaved in a wider range of σ, δ in bifurcation diagrams.

5. REFERENCE

1. Dowell, E.H., "Flutter of a buckled plate as an example of chaotic motion of a deterministic autonomous system", ***Journal of Sound and Vibration***, Vol. 85, No. 3, (1982), 333-344.
2. Fazelzadeh, S.A., "Chaotic behavior of nonlinear curved-panel in a supersonic flow", ***Dynamics of Continuous Discrete and Impulsive Systems Series B***, Vol. 14, No. 6, (2007), 793-810.
3. Yeh, Y.-L. and Lai, H.-Y., "Chaotic and bifurcation dynamics for a simply supported rectangular plate of thermo-mechanical coupling in large deflection", ***Chaos, Solitons & Fractals***, Vol. 13, No. 7, (2002), 1493-1506.
4. Turhan, O. and Bulut, G., "On nonlinear vibrations of a rotating beam", ***Journal of Sound and Vibration***, Vol. 322, No. 1, (2009), 314-335.
5. Abolghasemi, M. and Jalali, M., "Attractors of a rotating viscoelastic beam", ***International Journal of Non-Linear Mechanics***, Vol. 38, No. 5, (2003), 739-751.
6. Pan, L., Qiao, N., Lin, W. and Liang, Y., "Stability and local bifurcation in a simply-supported beam carrying a moving mass", ***Acta Mechanica Solida Sinica***, Vol. 20, No. 2, (2007), 123-129.
7. Gutschmidt, S. and Gottlieb, O., "Bifurcations and loss of orbital stability in nonlinear viscoelastic beam arrays subject to parametric actuation", ***Journal of Sound and Vibration***, Vol. 329, No. 18, (2010), 3835-3855.
8. Paolone, A., Vasta, M. and Luongo, A., "Flexural–torsional bifurcations of a cantilever beam under potential and circulatory forces ii. Post-critical analysis", ***International Journal of Non-Linear Mechanics***, Vol. 41, No. 4, (2006), 595-604.
9. Cao, D. and Zhang, W., "Global bifurcations and chaotic dynamics for a string-beam coupled system", ***Chaos, Solitons & Fractals***, Vol. 37, No. 3, (2008), 858-875.
10. Goyal, V.K. and Kapania, R.K., "Dynamic stability of laminated beams subjected to nonconservative loading", ***Thin-Walled Structures***, Vol. 46, No. 12, (2008), 1359-1369.
11. Di Egidio, A., Luongo, A. and Paolone, A., "Linear and non-linear interactions between static and dynamic bifurcations of damped planar beams", ***International Journal of Non-Linear Mechanics***, Vol. 42, No. 1, (2007), 88-98.
12. Kim, N.-I., "Dynamic stability behavior of damped laminated beam subjected to uniformly distributed subtangential forces", ***Composite Structures***, Vol. 92, No. 11, (2010), 2768-2780.
13. Luongo, A. and D'Annibale, F., "Double zero bifurcation of non-linear viscoelastic beams under conservative and non-conservative loads", ***International Journal of Non-Linear Mechanics***, Vol. 55, No., (2013), 128-139.
14. Daqaq, M.F., Alhazza, K.A. and Arafat, H.N., "Non-linear vibrations of cantilever beams with feedback delays", ***International Journal of Non-Linear Mechanics***, Vol. 43, No. 9, (2008), 962-978.
15. Lacarbonara, W., Arafat, H.N. and Nayfeh, A.H., "Non-linear interactions in imperfect beams at veering", ***International Journal of Non-Linear Mechanics***, Vol. 40, No. 7, (2005), 987-1003.
16. Mobki, H., Rezazadeh, G., Sadeghi, M., Vakili-Tahami, F. and Seyyed-Fakhrabadi, M.-M., "A comprehensive study of stability in an electro-statically actuated micro-beam", ***International Journal of Non-Linear Mechanics***, Vol. 48, No., (2013), 78-85.
17. Yang, J., Hu, Y. and Kitipornchai, S., "Electro-dynamic behavior of an electrically actuated micro-beam: Effects of initial curvature and nonlinear deformation", ***Computers & Structures***, Vol. 96, (2012), 25-33.
18. Pai, P.F. and Nayfeh, A.H., "Three-dimensional nonlinear vibrations of composite beams—ii. Flapwise excitations", ***Nonlinear Dynamics***, Vol. 2, No. 1, (1991), 1-34.
19. Arafat, H.N., "Nonlinear response of cantilever beams", Virginia Polytechnic Institute and State University, (1999),
20. Eftekhari, M., Mahzoon, M. and Ziaei-Rad, S., "Effect of added tip mass on the nonlinear flapwise and chordwise vibration of cantilever composite beam under base excitation", ***International Journal of Structural Stability and Dynamics***, Vol. 12, No. 02, (2012), 285-310.

Post-critical Behavior of Three-dimensional Composite Beams Near the Autoparametric Resonance under Flapwise Excitation

M. Eftekhari*

Department of Mechanical Engineering, Shahid Bahonar University of Kerman, Kerman, Iran

P A P E R I N F O

Paper history:
Received 21 December 2015
Received in revised form 09 March 2016
Accepted 02 June 2016

Keywords:
Composite Beam
Flapwise Excitation
Autoparametric Resonance
Periodic Motions

چکیده

آنالیز دوشاخه ای شدن یک تیر کامپوزیت متقارن که تحت تحریک جانبی پایه قرار گرفته است در حالتی که تشدید داخلی در تیر وجود دارد و نسبت تشدید داخلی جهت جانبی و عرضی تیر برابر ۱ به ۲ است مورد مطالعه قرار گرفته است. نتایج عددی دو شاخه ای شدن از حل معادلات مدولاسیون استخراج شده است. در کارهای قبلی، معادلات مدولاسیون خاصیت تقارن را از خود نشان نمی دادند و معادلات اصلاح شده با خاصیت تقارن در این مقاله مطالعه می شود. این نتایج به صورت دیاگرامهای پاسخ زمانی،صفحه فاز و دیاگرام دو شاخه ای نگاشت پوانکاره می باشد. نتایج نشان می دهند که حرکتهای پریودیک با یک و یا چند سیکل، پرش و حرکت پایدار در نزدیکی پارامتر تنظیم فرکانس تحریک جانبی و پارامتر تنظیم تشدید داخلی ظاهر می شود

***doi**: 10.5829/idosi.ije.2016.29.06c.00*